Electronic Supporting Information

Double Rare-Earth Nanothermometer in Aqueous Media: Opening the Third Optical Transparency Window to Temperature Sensing

A. Skripka,[a] A. Benayas,[a] R. Marin,[a,b] P. Canton, [b] E. Hemmer[a] and F. Vetrone[*ac]

[a]*Institut National de la Recherche Scientifique, Centre Énergie Matériaux Télécommunications, Université du Québec, Varennes, Québec J3X 1S2, Canada.*
E-mail: vetrone@emt.inrs.ca

[b]*Dipartimento di Scienze Molecolari e Nanosistemi, Università Ca' Foscari di Venezia, Via Torino 155/b, I-30170 Venezia-Mestre, Italy*

[c]*Centre for Self-Assembled Chemical Structures, McGill University, Montréal, Québec H3A 2K6, Canada*

Experimental section: synthesis, surface modification, structural and optical characterization

Precursor synthesis

Core/shell/shell/shell $NaGdF_4$: 2 mol% Er^{3+}, 5 mol% Ho^{3+}, 20 mol% Yb^{3+} / $NaGdF_4$: 10 mol% Yb^{3+} / $NaGdF_4$: 5 mol% Nd^{3+}, 20 mol% Yb^{3+} / $NaGdF_4$ NPs (T^{NIR}-NPs) were synthesized via the thermal decomposition method.[1] Precursors for the core were prepared by mixing 0.9125 mmol of Gd_2O_3 (99.99+ %), 0.25 mmol Yb_2O_3 (99.99+ %), 0.025 mmol Er_2O_3 (99.99+ %) and 0.0625 mmol Ho_2O_3 (99.99+ %) with 5 mL trifluoroacetic acid (99 %) and 5 mL of distilled water in a 50 mL three-neck round bottom flask. The mixture was then refluxed under vigorous stirring at 80 ºC until a clear solution was obtained, at which point the temperature was decreased to 60 ºC in order to slowly evaporate residual trifluoroacetic acid and water. Shell #1, #2, and #3 precursors were prepared separately in analogy to the core precursor. Shell #1 precursor: 1.125 mmol Gd_2O_3 (99.99+ %), 0.125 mmol Yb_2O_3 (99.99+ %). Shell #2 precursor: 0.975 mmol Gd_2O_3 (99.99+ %), 0.25 mmol Yb_2O_3 (99.99+ %), 0.0625 mmol Nd_2O_3 (99.99+ %). Shell #3 precursor: 1.25 mmol Gd_2O_3 (99.99+ %). All precursors were obtained as solid dried materials and were used for the T^{NIR}-NPs synthesis without further purification. All materials involved in the precursor synthesis were obtained from Alfa Aesar, USA, and were used without further purification.

Synthesis of T^{NIR}-NPs

<u>$NaGdF_4$: Er^{3+}, Ho^{3+}, Yb^{3+} core.</u> An initial mixture of 12.5 mL each of oleic acid (90 %, Alfa Aesar, USA) and 1-octadecene (90 %, Alfa Aesar, USA) was prepared in a 100 mL three-neck round bottom flask (Solution A). Seperately, 2.5 mmol of sodium trifluoroacetate (98 %, Alfa Aesar, USA) were added to the dried core precursor together with 7.5 mL each of oleic acid and 1-octadecene (Solution B). Both solutions A and B were degassed at 145 ºC under vacuum with magnetic stirring for 30 min. After degassing, solution A was placed under inert Ar atmosphere and the temperature was slowly raised to 315 ºC. Solution B was then injected into the reaction

vessel containing solution A using a syringe and pump system (Harvard Apparatus Pump 11 Elite, USA) at a 1.5 mL/min injection rate. The mixture was left at 315 ºC under vigorous stirring for 60 min.

Core/$NaGdF_4$: Yb^{3+} shell #1. A solution of shell #1 precursor and 2.5 mmol of sodium trifluoroacetate dissolved in 4 mL each of oleic acid and 1-octadecene (Solution C, degassed at 145 ºC under vacuum with magnetic stirring for 30 min) was injected into the reaction vessel at 1.5 mL/min injection rate. The mixture was left at 315 ºC under vigorous stirring for 60 min to form the $NaGdF_4$: Yb^{3+} shell #1 around the previously formed core of T^{NIR}-NPs.

Core/shell #1/$NaGdF_4$: Nd^{3+}, Yb^{3+} shell #2. A solution of shell #2 precursor and 2.5 mmol of sodium trifluoroacetate dissolved in 4 mL each of oleic acid and 1-octadecene (Solution D, degassed at 145 ºC under vacuum with magnetic stirring for 30 min) was injected into the reaction vessel at 1.5 mL/min injection rate. The mixture was left at 315 ºC under vigorous stirring for 60 min to form the $NaGdF_4$: Nd^{3+}, Yb^{3+} shell #2 around Core/shell #1.

Core/shell #1/shell #2/$NaGdF_4$. Finally, solution E (undoped shell #3 precursor, 2.5 mmol sodium trifluoroacetate, 4 mL oleic acid, 4 mL 1-octadecene, degassed at 145 ºC under vacuum with magnetic stirring for 30 min) was injected at 1.5 mL/min injection rate resulting in the growth of the outer passivating shell #3.

After a total of 4 h of reaction time, the final mixture was allowed to cool down to room temperature, maintaining the magnetic stirring and Ar atmosphere. Subsequently, the oleate-capped core/shell/shell/shell T^{NIR}-NPs were precipitated with ethanol and recollected via centrifugation at 6000 RPM for 15 min. The obtained T^{NIR}-NPs were washed twice with a mixture of hexane/ethanol (1/4 v/v) and precipitated via centrifugation. Finally, the oleate-capped T^{NIR}-NPs were redispersed in hexane for storage and physical characterization.

T^{NIR}-NPs transfer to water via phospholipid coating

Oleate-capped T^{NIR}-NPs were transferred into an aqueous environment (T^{NIR}-*aq*NPs) following a modified, previously reported, phospholipid coating method.[2] 50 mg of T^{NIR}-NPs were redispersed in 4 mL of chloroform (99.9 %, Sigma Aldrich, Germany) together with 5.6 mg (2 μmol) of 1,2-dioleoyl-*sn*-glycero-3-phosphoethanolamine-N-[methoxy(polyethylene glycol)-2000] (PEG-DOPE) phospholipids (Avanti Polar Lipids, Inc., USA). The content was lightly swirled by hand, shortly after following chloroform evaporation at 45 ºC under inert Ar atmosphere resulting in a dry phospholipid film containing the NPs. Subsequently, distilled water (5 mL) was added in order to hydrate the dry phospholipid film under sonication at 65 ºC temperature for 60 min. Finally, the mixture was successively passed through 0.45 μm and 0.2 μm filters to remove large phospholipid and NP-phospholipid structures.

Structural characterization of T^{NIR}-(*aq*)NPs

The crystallinity and phase of the core-only, core/shell #1, core/shell #1/shell #2, and core/shell #1/shell #2/shell #3 structures were determined via X-ray powder diffraction (XRD) analysis on a Bruker D8 Advance Diffractometer using CuKα radiation. The morphology and size distribution of the core-only, core/shell #1, core/shell #1/shell #2, and core/shell #1/shell #2/shell #3 NPs were further investigated by transmission electron microscopy (TEM, Philips Tecnai 12). The particle size was determined from TEM images using ImageJ

software with set size of 400 particles per core-only, core/shell #1, core/shell #1/shell #2, and core/shell #1/shell #2/shell #3 samples.

Fourier transform infrared (FTIR) spectra of the synthesized oleate-capped T^{NIR}-NPs, ligand-free T^{NIR}-NPs (ligand removal was achieved according to previously reported method[3]), PEG-DOPE micelle encapsulated T^{NIR}-*aq*NPs, pure PEG-DOPE, and pure oleic acid were recorded with a ThermoFisher Scientific Nicolet 6700 FTIR spectrometer. The specimens were prepared mixing together few milligrams of dried samples, or a drop of liquid samples, with KBr (FTIR grade, Alfa Aesar, USA) and pressing them in tablets. TEM images of PEG-DOPE coated T^{NIR}-*aq*NPs were obtained with a FEI Tecnai G2 spirit Twin microscope.

Optical characterization of T^{NIR}-(*aq*)NPs and their thermal response in NIR

Upconversion and NIR emission spectra T^{NIR}-(*aq*)NPs (in hexane or water) were obtained at room temperature under laser diode excitation of 806 nm (140 W/cm^2; Lumics, Germany). The upconversion emission was collected using a lens at a 90º angle from the excitation beam and recorded with an Avaspec-ULS2048L spectrometer (Avantes, Netherlands). The optical path configuration of 180º angle between the excitation and collection pathways was utilized for the NIR emission measurements, which was recorded with a Shamrock 500i monochromator (Andor, Ireland) equipped with an iDus InGaAs 1.7 NIR detector (Andor, Ireland). In order to remove any stray light from the excitation source a short-pass 785 nm and a long-pass 980 nm filters (Semrock, Inc., USA) were used for the visible and NIR range spectrum acquisitions, respectively. T^{NIR}-(*aq*)NPs in water and hexane were maintained at approximate 1 wt% concentration for all measurements.

NIR imaging through chicken breast tissue was carried out by exciting (806 nm; 11 W/cm^2) the dry pellet of T^{NIR}-*aq*NPs or colloidal suspension of T^{NIR}-*aq*NPs in a 0.2 mm optical path length glass capillary (Electron Microscopy Sciences, USA). The chicken breast tissue was placed between the sample and NIR imaging camera (XEVA-1781, Xenics, Belgium), emitted light in the 1100 – 1700 nm spectral range was selected either by long-pass 1150 nm (1150LP) or 1450 nm (1450LP) filters (Thorlabs, USA).

The thermal response of T^{NIR}-NPs and T^{NIR}-*aq*NPs was measured in the 20 to 50 ºC temperature range at 5 ºC increments. The temperature was changed using a temperature controlled cuvette holder (qpod 2e by Quantum Northwest, Washington, USA). 10 min intervals were maintained between the measurements in order to assure the stabilization of set temperature across the sample. The nanothermometric properties of the T^{NIR}-*aq*NPs were determined from a triplet of heating-cooling cycles.

Nanothermometric properties (relative thermal sensitivity S_r) were additionally tested in Dulbecco's modified Eagle's cell culturing medium containing 10% fetal bovine serum (PAN-Biotech, Germany) and different normal/heavy water (99.98 at%; Sigma Aldrich, Germany) ratios (4:0, 3:1, 2:2, 1:3).

Estimating nanothermometric performance of T^{NIR}-*aq*NPs

Luminescence intensity ratio (*LIR*) is estimated taking the ratio between the integrated intensities (I_1 and I_2) of the temperature sensitive emission bands (here I_1 - Ho^{3+} 1.18 μm or Er^{3+} 1.55 μm bands and I_2 - Nd^{3+} 1.34 μm band), at each temperature value:

$$LIR = \frac{I_1}{I_2}$$

Subsequently, the relative thermal sensitivity (S_r) of the material is calculated as:

$$S_r = \frac{1}{LIR}\frac{\partial LIR}{\partial T}$$

The temperature uncertainty (δT) is given by:

$$\delta T = \frac{1}{S_r}\frac{\delta LIR}{LIR}$$

All of the respective error values for the determined parameters were found according to the error propagation rules.

Structural analysis of T^{NIR}-NPs

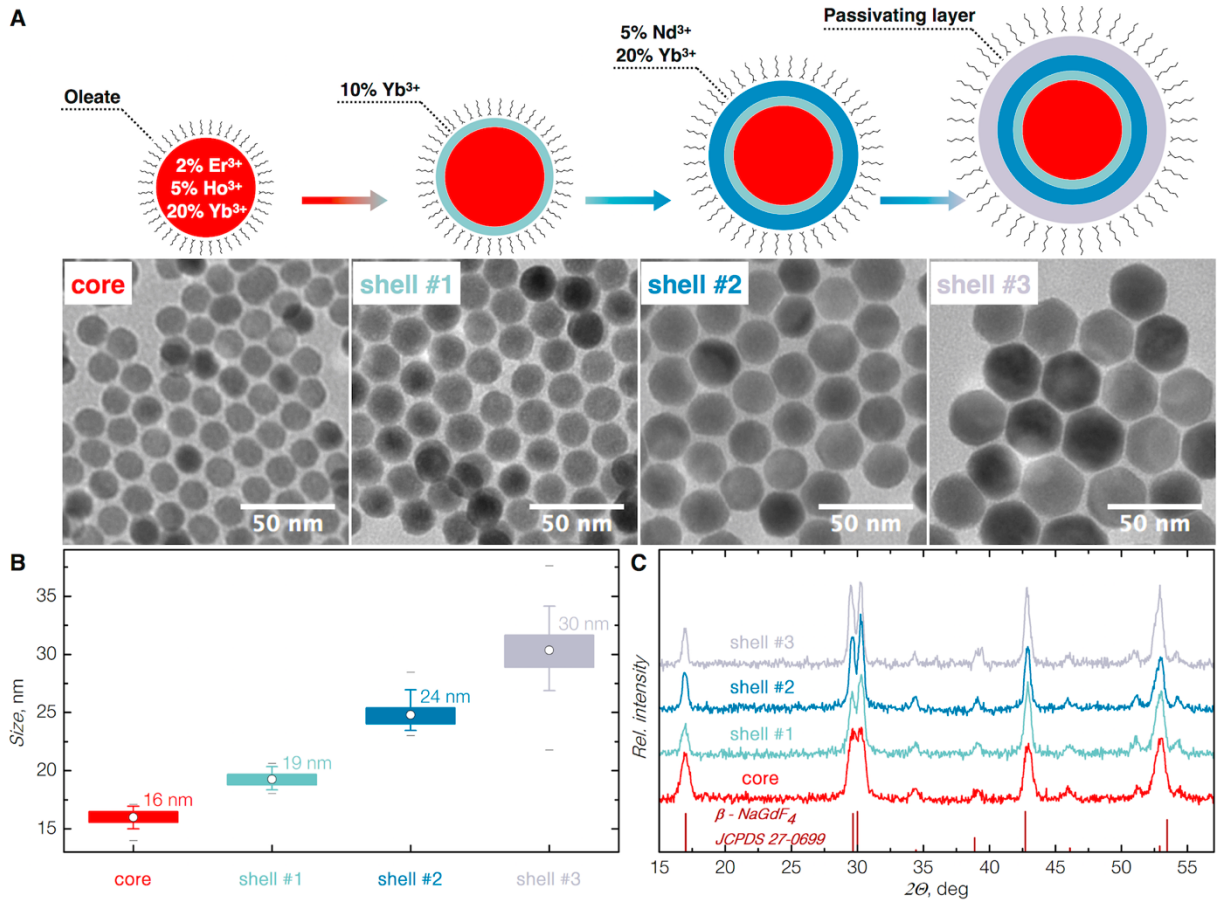

Figure S1. A — Multilayered $NaGdF_4$ T^{NIR}-NPs of 2 mol% Er^{3+}, 5 mol% Ho^{3+}, 20 mol% Yb^{3+} - core / 10 mol% Yb^{3+} - shell #1 / 5 mol% Nd^{3+}, 20 mol% Yb^{3+} - shell #2 and undoped (passivating layer) shell #3 were synthesized via thermal decomposition. The uniform growth of each nanoparticle's composing layer can be observed from the TEM images. B — Taking the set size of 400 particles per sample the average sizes were estimated as 16 nm - core, 19 nm - core/shell #1, 24 nm - core/shell #1/shell #2, and 30 nm - core/shell #1/shell #2/shell #3. As can be seen from the box plots of the particle size distribution, at each of the growth steps narrow and monodisperse size distribution is maintained with only slight broadening after the formation of the passivating layer - shell #3. Boxes denote 1st and 3rd quartiles, mean values are indicated as a circle, whiskers - 5th and 95th percentiles, minimum and maximum values are shown by the bars. C — X-ray powder diffraction patterns of core-only, core/shell #1, core/shell #1/shell #2, and core/shell #1/shell #2/shell #3 samples revealed pure hexagonal (β) phase crystallinity of each T^{NIR}-NPs composing layer.

Surface characterization of T^{NIR}-*aq*NPs

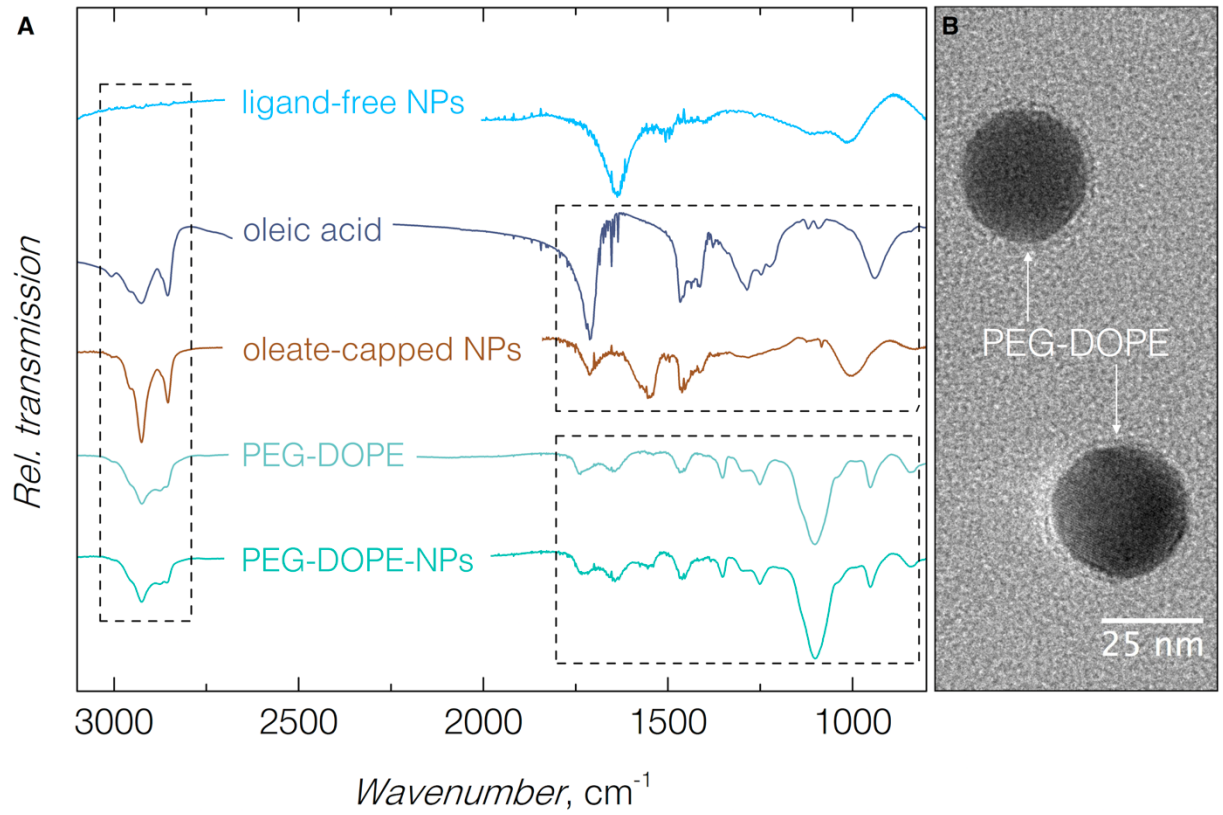

Figure S2. A — FTIR spectral analysis of PEG-DOPE modified T^{NIR}-*aq*NPs as compared to ligand-free and oleate-capped T^{NIR}-NPs. For the ease of the comparison, FTIR spectra of pure oleic acid and pure PEG-DOPE were also recorded. The change in the surface modification of the T^{NIR}-NPs is most clearly observed in the range of asymmetric and symmetric stretching of $-CH_2$ groups around 2900 cm^{-1}. Oleate-capped and PEG-DOPE modified T^{NIR}-(*aq*)NPs showed oleic acid and PEG-DOPE specific IR bands in the 1800 - 600 cm^{-1} region, while only the water IR band at around 1640 cm^{-1} is present in this region for ligand-free NPs. B — The T^{NIR}-NPs encapsulation in PEG-DOPE phospholipid micelles is directly observed from the high magnification TEM micrographs, where the PEG-DOPE corona surrounding the T^{NIR}-*aq*NPs can be seen.

Heat generation in water by laser irradiation

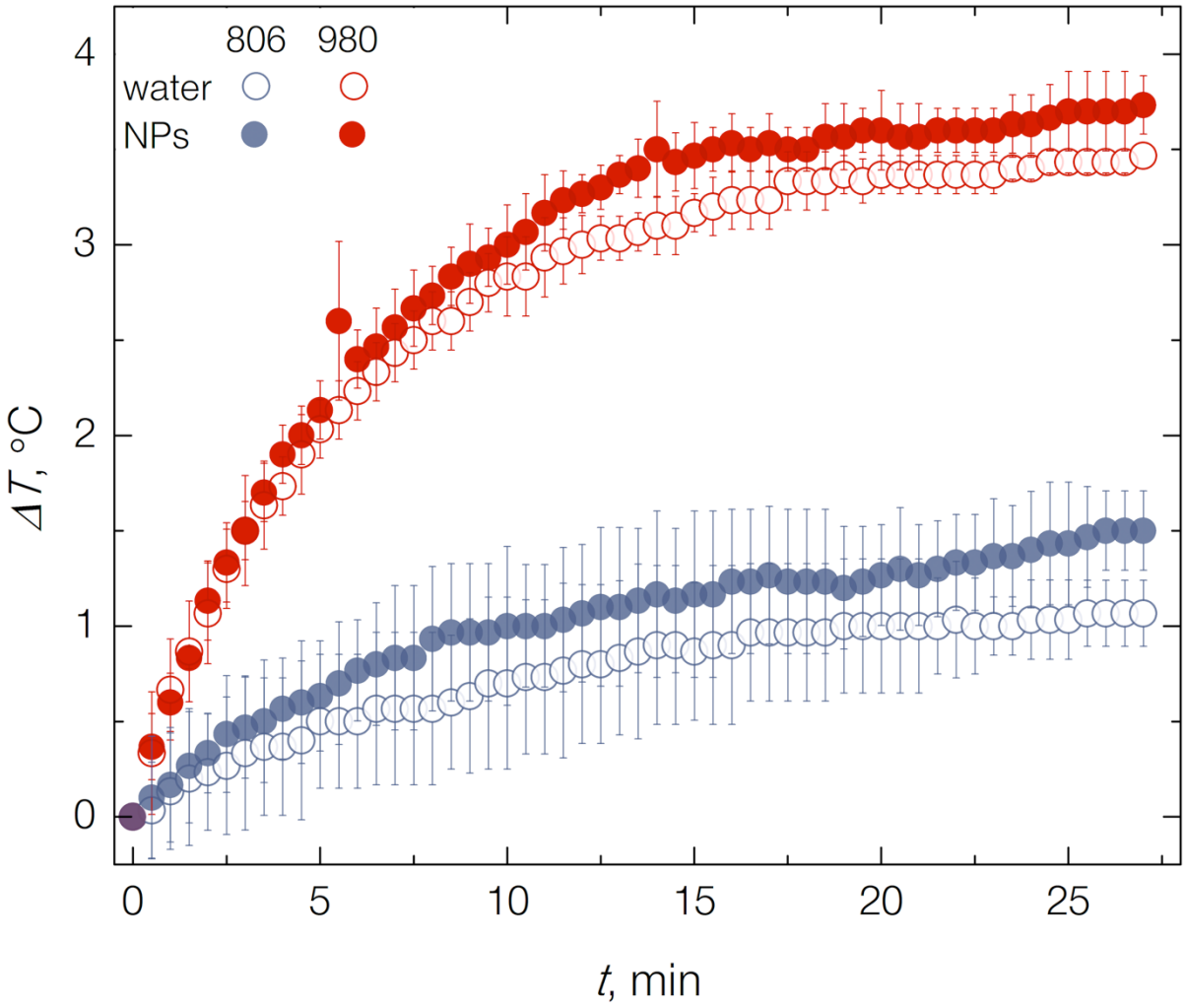

Figure S3. Relative temperature change of pure water (open circles) under 806 or 980 nm wavelength laser continuous irradiation (140 W/cm^2; corresponding to 190 mW) and in case of 1 wt% of T^{NIR}-*aq*NPs present in the medium (full circles). The temperature of pure water and the T^{NIR}-*aq*NPs colloidal solution increased by approximately 3.5 ºC when irradiated by 980 nm laser for longer than 25 min. In contrast, only a maximal increase of 1.5 ºC was observed in case of the T^{NIR}-*aq*NPs colloidal solution under 806 nm irradiation. Clearly, water absorption and subsequent energy dissipation in the form of heat is more pronounced for 980 nm wavelength irradiation, which under prolonged illumination can raise the local temperature high enough to induce a significant error in the temperature measurement or even undesired thermal damage to biological tissues.

Upconversion emission of T^{NIR}-*aq*NPs

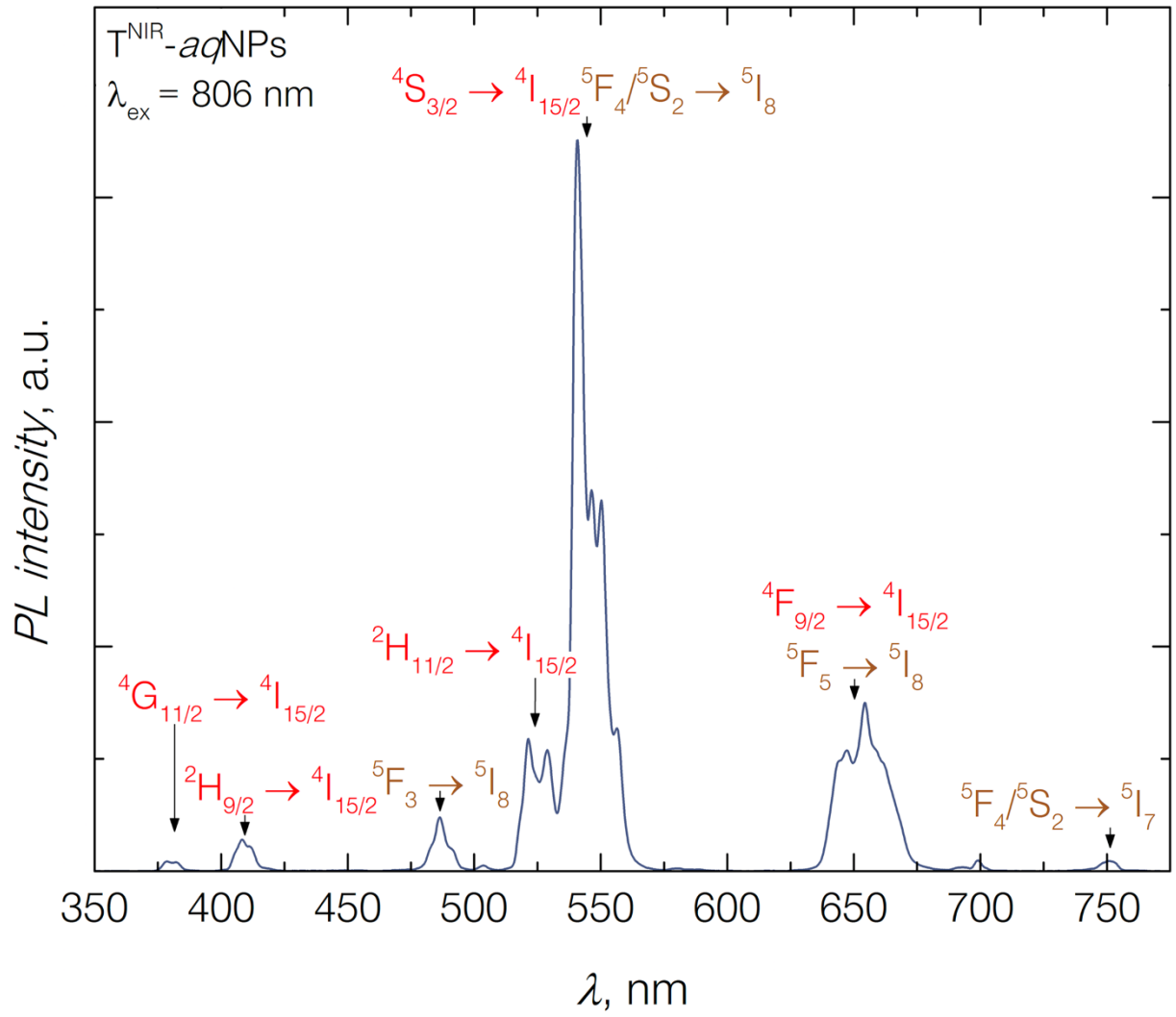

Figure S4. Water dispersible T^{NIR}-*aq*NPs, when excited by 806 nm irradiation, show a multitude of upconversion generated emission bands in the UV, visible, and even NIR spectral ranges. Emission bands at 380 ($^4G_{11/2} \rightarrow {}^4I_{15/2}$), 410 ($^2H_{9/2} \rightarrow {}^4I_{15/2}$), and 525 nm ($^2H_{11/2} \rightarrow {}^4I_{15/2}$) solely stem from the Er^{3+} ions, while Ho^{3+} specific upconversion bands are found around 486 ($^5F_3 \rightarrow {}^5I_8$) and 750 nm ($^5F_4/{}^5S_2 \rightarrow {}^5I_7$). The most intense upconversion emission bands at 540 (Er^{3+}: $^4S_{3/2} \rightarrow {}^4I_{15/2}$; Ho^{3+}: $^5F_4/{}^5S_2 \rightarrow {}^5I_8$) and 650 nm ($Er^{3+}$: $^4F_{9/2} \rightarrow {}^4I_{15/2}$; Ho^{3+}: $^5F_5 \rightarrow {}^5I_8$) appear from both ions emitting in nearly the same spectral position.

NIR emission of T^{NIR}-*aq*NPs through optically scattering and absorbing media

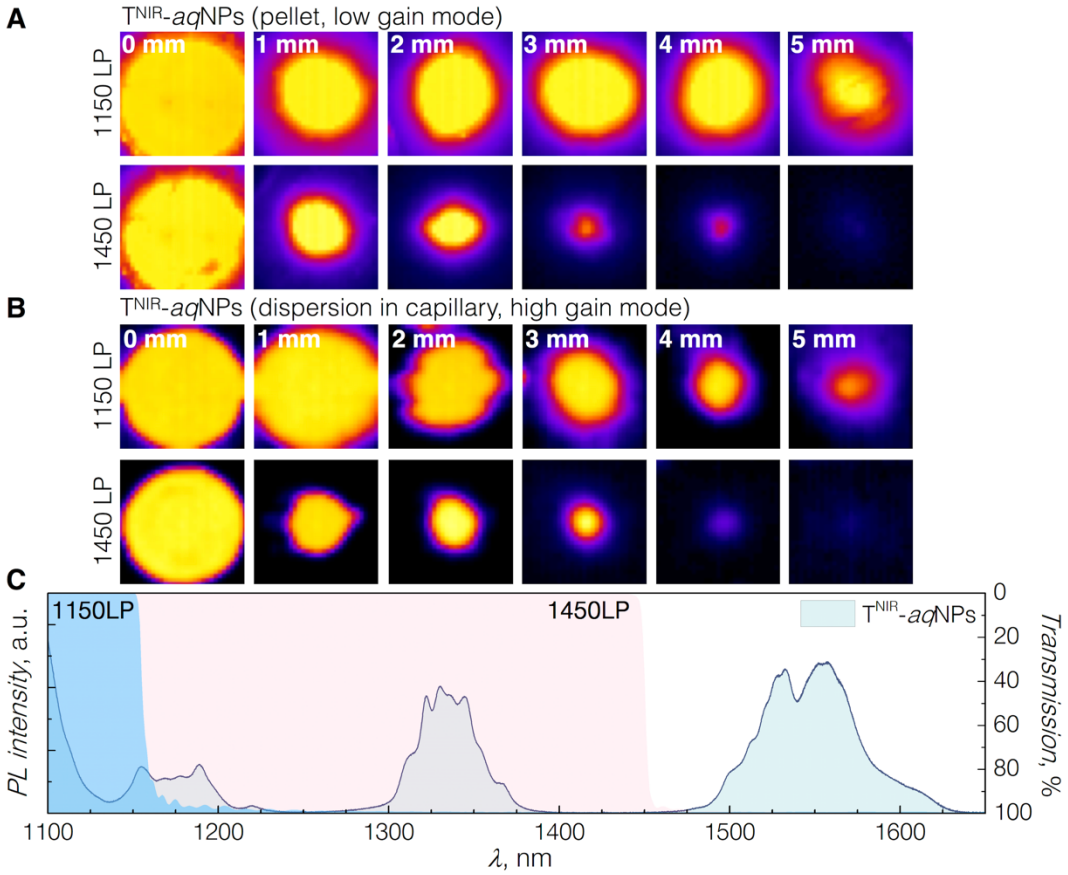

Figure S5. A, B - NIR emission observed from T^{NIR}-*aq*NPs after propagation through chicken breast tissue of 1 to 5 mm of thickness (A - pellet, B - 1 wt% colloidal dispersion in a glass capillary, 806 nm excitation of 11 W/cm^2). Utilizing a set of 1150LP and 1450LP filters, it can be seen that 1.55 μm emission of Er^{3+} allows to achieve higher spatial resolution due to reduced light scattering. C – Representative spectrum of T^{NIR}-*aq*NPs overlapped with the transmission of 1150LP and 1450LP filters utilized for the acquisition of the corresponding images in A and B. Dataset for the transmission of filters is obtained from thorlabs.com.

LIR of T^{NIR}-*aq*NPs in water with respect to temperature changes

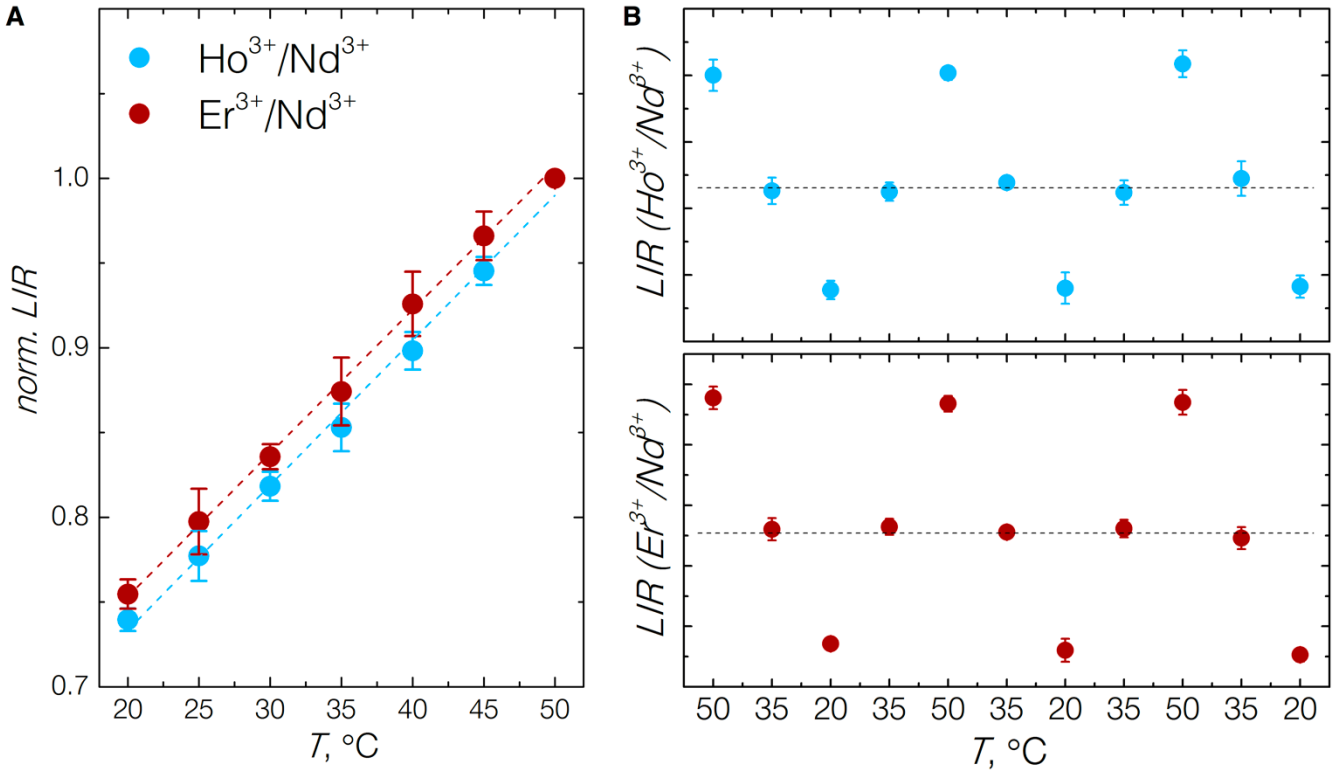

Figure S6. A - (Normalized for ease of comparison) LIR (Ho^{3+}/Nd^{3+}) and LIR (Er^{3+}/Nd^{3+}) from T^{NIR}-*aq*NPs are linearly dependent on the temperature of the surrounding environment. B - Under multiple heating and cooling cycles, the LIR values of Ho^{3+}/Nd^{3+} and Er^{3+}/Nd^{3+} are reproducible up to 99 % and colloidal stability of the T^{NIR}-*aq*NPs remains unaffected.

NIR emission of T^{NIR}-NPs in hexane with respect to temperature changes

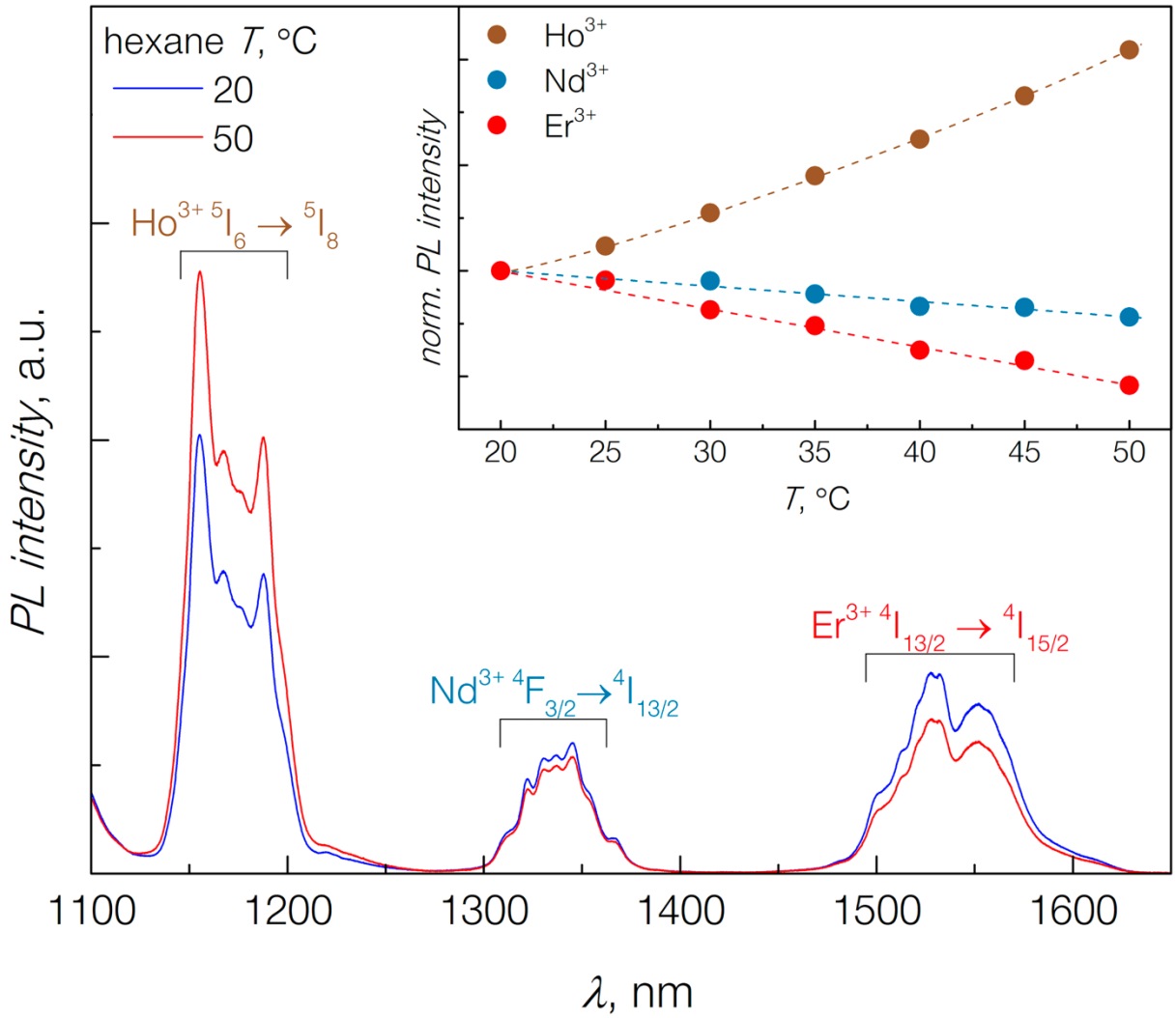

Figure S7. T^{NIR}-NPs dispersed in hexane and excited with 806 nm irradiation (140 W/cm^2) show three distinct NIR emission bands of Ho^{3+} (1.18 μm), Nd^{3+} (1.34 μm), and Er^{3+} (1.55 μm) ions. A change in the temperature (20 – 50 ºC) of the suspension leads to a significant increase of the Ho^{3+} emission intensity, while both Nd^{3+} and Er^{3+} emissions decrease. The inset depicts the relative changes of each of the emission band intensities with respect to the temperature variation. Dashed lines are used solely for the guidance purpose of the eye.

NIR emission of T^{NIR}-*aq*NPs in normal/heavy water mixtures and cell culturing medium

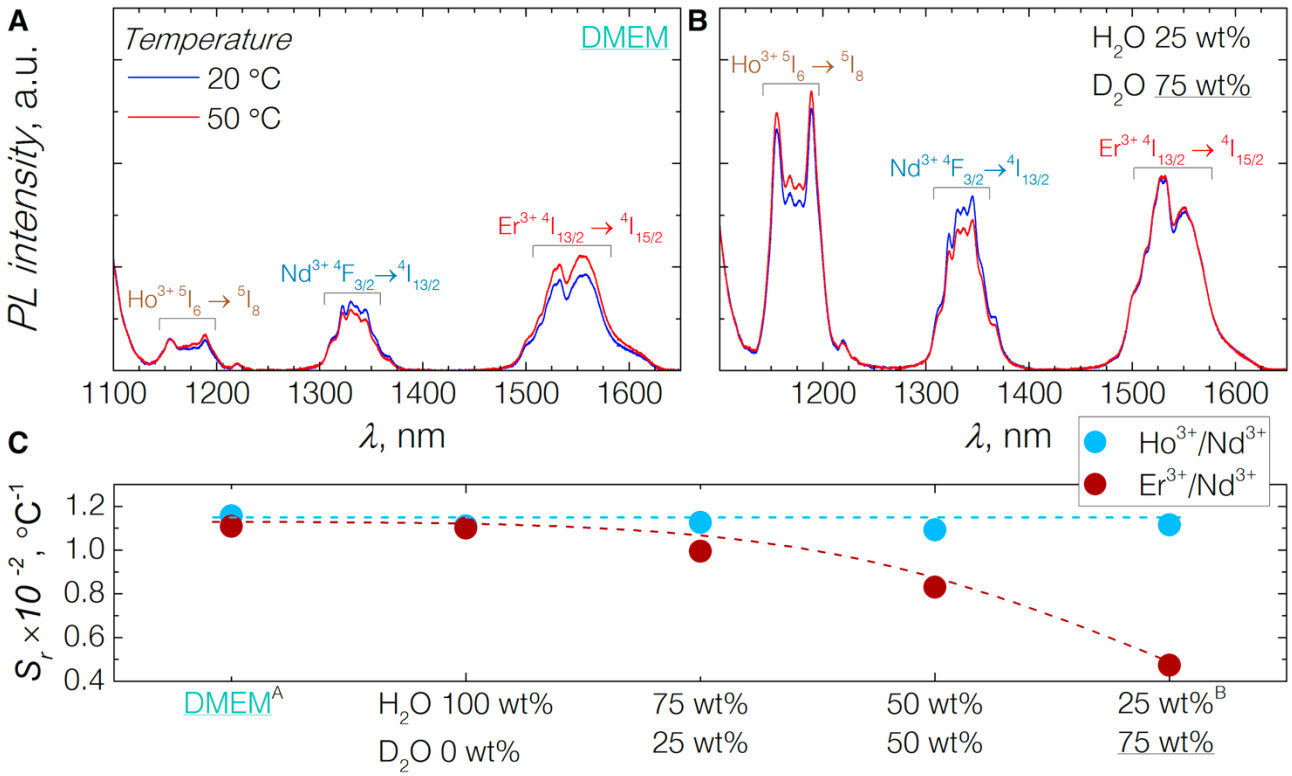

Figure S8. Representative spectra of A - T^{NIR}-*aq*NPs colloidal DMEM and B - H_2O/D_2O (25 wt%/75 wt%) solutions at 20 and 50 ºC. Identical behavior of T^{NIR}-*aq*NPs in DMEM as in control distilled water solution (Fig. 2, main article text) is observed, while increased amounts of D_2O result in an Er^{3+} 1.55 μm band invariance to the local temperature. C - Relative thermal sensitivity S_r of T^{NIR}-*aq*NPs in cell culturing medium (DMEM; supplemented with 10 % fetal bovine serum) and normal/heavy water mixtures at different ratio. Dashed lines in the figure serve the purpose to guide the eye. The T^{NIR}-*aq*NPs demonstrate a stable nanothermometric performance across most of the tested conditions. A deviation of the S_r in case of Er^{3+}/Nd^{3+} was observed when the relative heavy water amount constituted the majority of the total solution (75 wt%). In this case, the temperature associated NIR band intensity changes were approaching the situation observed for T^{NIR}-NPs in hexane.

Table S1. Comparison of RENP nanothermometers operating in the NIR (1000 – 1700 nm) spectral range.

Nanoparticles	***NP size* (nm)***	λ_{ex} (nm)	λ_{em} *used for LIR* (nm)	***Medium***	S_r (* 10^{-2} $^oC^{-1}$)#	***Reference*** **
LaF_3:Nd^{3+},Yb^{3+}	24	790	1000/1300	Aqueous dispersion	0.41 - 0.337 @ 283 - 323 K	E. C. Ximendes et al. (*Nano Lett.* 2016)[5]
Gd_2O_3:Nd^{3+} nanorods	13.5 x 91.0 (diam. x length)	580	782-865/865-925	Dried powders	1.5 - 1.1 @ 295 - 315 K	S. Balabhadra et al. (*Nanoscale 2015*)[23]
$NaYF_4$:Er:Yb@$NaYF_4$:Nd:Yb	~ 30[b]	808	980/1060	Dried powders	0.20 - 1.50 @ 280 - 340 K	L. Marciniak et al. (*Nanoscale* 2016)[23]
$LiLaP_4O_{12}$ Cr^{3+},Nd^{3+}	19	665	830/1050	Dried powders	3.70 - 4.89 @ 273 - 323 K	L. Marciniak et al. (*J. Mat. Chem. C* 2016)[23]
$NaGdF_4$:Nd^{3+} & PbS/CdS/ZnS@ PLGA	150	808	1060/1250	Aqueous dispersion	1.00 - 2.50 @ 283 - 328 K	E. N. Cerón et al. (*Adv. Mat.* 2015)[26]
T^{NIR}-*aq*NPs[a]	30	806	1150/1330 1330/1550	Aqueous dispersion	1.16 - 0.86 @ 293 - 323 K 1.10 - 0.83 @ 293 - 323 K	This work

* TEM estimates of average NP size.

Relative thermal sensitivity in the biologically relevant temperature range.

** References are numbered according to their appearance in the main text.

[a] $NaGdF_4$: Er^{3+}, Ho^{3+}, Yb^{3+}@$NaGdF_4$: Yb^{3+}@$NaGdF_4$: Nd^{3+}, Yb^{3+}@$NaGdF_4$ coated with PEG-DOPE.

[b] Size was estimated manually from the available TEM images, as it is not indicated by authors in the article.

References

[1] Boyer, J. C.; Vetrone, F.; Cuccia, L. A.; Capobianco, J. A., Synthesis of colloidal upconverting $NaYF_4$ nanocrystals doped with Er^{3+}, Yb^{3+} and Tm^{3+}, Yb^{3+} via thermal decomposition of lanthanide trifluoroacetate precursors. *J. Am. Chem. Soc.* **2006,** *128* (23), 7444-5.

[2] Dubertret, B.; Skourides, P.; Norris, D. J.; Noireaux, V.; Brivanlou, A. H.; Libchaber, A., In vivo imaging of quantum dots encapsulated in phospholipid micelles. *Science* **2002,** *298* (5599), 1759-62.

[3] Bogdan, N.; Vetrone, F.; Ozin, G. A.; Capobianco, J. A., Synthesis of ligand-free colloidally stable water dispersible brightly luminescent lanthanide-doped upconverting nanoparticles. *Nano Lett.* **2011,** *11* (2), 835-40.